We are IntechOpen,
the world's leading publisher of
Open Access books
Built by scientists, for scientists

6,900
Open access books available

185,000
International authors and editors

200M
Downloads

154
Countries delivered to

Our authors are among the

TOP 1%
most cited scientists

12.2%
Contributors from top 500 universities

CLARIVATE ANALYTICS
BOOK
CITATION
INDEX
INDEXED

WEB OF SCIENCE™

Selection of our books indexed in the Book Citation Index
in Web of Science™ Core Collection (BKCI)

Interested in publishing with us?
Contact book.department@intechopen.com

Time and Light

Igor Peshko

Additional information is available at the end of the chapter

1. Introduction

1.1. From seconds to attoseconds

This book is devoted to Laser Pulses. In the modern laser world, the word "Pulse" covers pulse durations from microseconds (free-running laser) to tens of femtoseconds (1fs is 10^{-15} s) (mode-locked laser). It is possible to generate attosecond pulses (1as is 10^{-18} s) by using non-linear processes. Recently, a new time range was discussed in publications: zeptosecond (1zs is 10^{-21} s). To generate pulses from milliseconds to femtoseconds, hundreds of different laser systems have been developed. They can typically generate pulses of specific durations, which are due to laser principles of operation, specific construction, parameters of gain medium, type of modulator, and so on.

In the solid-state free-running laser the parameters of the electromagnetic field interaction process with an inversed population of the gain medium play a dominant role in shaping the laser spikes. These characteristic parameters limit the pulse duration from the long side of the range. A chaotic sequence of such spikes can be as long as the pumping source could effectively excite the gain medium. In some technological applications this can be hundreds of milliseconds envelop. To achieve laser pulse duration of a few seconds, it is necessary to use for modulation the processes with characteristic times of the same order of magnitude. On the short side of achievable durations, another limitation exists. At certain conditions, waves, interacting with solids, can shape a single peak of energy, propagating "alone". In optics, such a single wave is called a "soliton". A tsunami is an example of a mechanical soliton. To propagate in a crystal, an "optical tsunami" can excite the medium and get back the energy at some conditions. In a vacuum, there is no medium that can accumulate energy and support existence of a relatively short, lossless wave. Hence, in a vacuum, a single pulse could be shaped as a wave-package, which is a result of interference of many independent electromagnetic waves, propagating co-axially in the same direction. Since light is an electromagnetic wave repeatable in space and time, a single wave period with minimal

length (among all present in the wave set) is the minimal possible duration of an energy pack. Out of the pulse, the negative interference suppresses the energy presence.

Pulse measurement techniques were being developed together with each type of laser and are based on principles depending on the specific range of pulse duration. The shorter the achieved pulse durations, the more difficult the problem of how to measure such pulses. The answer is inside the laser pulses. Light itself contains information about Time.

In summary, we can say that lasers, generating "light in time", combine these two categories as light is a periodical, cyclic process and can be a measure of time and of length. Since this is an introductive chapter, let us consider some historical milestones on the way of Time/Light understanding first.

1.2. In the past

On the way of analysing and understanding Nature, ancient scientists interpreted Light and Time as two absolutely different categories. To this day, it is not clear what Time is - is it a characteristic of processes, or an independently existing parameter? Theoretical physics operates with 4D space: 3 space coordinates and the fourth as time. To measure any distance, a researcher can compare some etalon of length with the object of interest. However, historically, the etalon of length was voluntarily chosen: 1 m is not a "natural" unit of length. At the same time, the light specific wavelength is a natural, repeatable etalon of length. The same is true for time – any process running with macro-objects being involved is just approximately repeatable. Since the speed of light (in vacuum) is the same everywhere, it can be used for measuring time and length: the same number of light waves with specific length corresponds to the same distance in any corner of the Universe – at least, we think so.

If existence of Light is absolutely evident, what supposed to be Time is not very clear until now. A lot of serious discussion and speculation was done but the problem still has to be solved. Time is not a single example of a "questionable" phenomenon. Very often, scientists propose a phantom model that helps make a very helpful device or theoretical approximation. The most popular parameter in optics - "index of refraction" - is probably the most investigated phenomenon that does not exist in Nature at all. This is a very useful model that helps provide theoretical research and find technological solutions in the fields of optics, photonics, and other related areas of activity.

We see or measure light as a result of photon interaction with more "solid" matter: atoms in our eyes or other detectors. In the case of time, the situation is more complicated. Since the early ages of humanity, people observed some regularly repeatable events, like day-night, winter-summer, etc., that, de-facto, were connected with complete or partial appearance and disappearance of light. Probably the first instrument for estimation of day time was the sundial – a vertically installed bar that showed the time period relative to specific points when the position of the sun over the horizon is maximally high and bar shadow is maximally short (midday). However, in cloudy days or at night, the system was useless. The

next step in time measuring devices was the sand or water clock (Clepsydra): a spring of water or sands running through a small hole filled or emptied some calibrated tank. This is the most ancient experimental 3D demonstration of the basic formula of time: $T = M/R$ where M is mass and R is rate of mass changes. A very well-known 1D variant of this formula reads: $T = L$ (length)$/V$ (velocity). In case of a "floating clock", M is the total amount of water in the tank and R is the amount of water that drops through the hole during a unit of time. In this case, to build two identical clocks, one needs to make holes with ideally identical cross-sections. So, accuracy of time measurement is linked to accuracy of length measurement.

The next step was a mechanical clock with a pendulum. This device periodically transforms kinetic energy of motion into potential energy of a pendulum in the gravitation field. The electronic clocks use a periodic process of transformation of the electrical energy stored in a capacitor into magnetic energy of a coil. Each repeatable process can be used for measuring time. This could be a planet's rotation around a star, or a planet's rotation around its own axis, or mechanical vibrations – sound, or electromagnetic waves – light.

As of today, the history of pulsed lasers spans about 50 years. Hundreds of books devoted to this subject have been published during this period. More and more techniques go to practical use every year. Shorter and shorter pulses are routinely applicable. New spectral ranges, like deep UV, middle and far IR, including TeraHertz bands became a reality. This book demonstrates new achievements in theory, experiments, and commercial applications of pulsed lasers.

1.3. What is this chapter about?

Until the mid-eighties of the previous century, most of the lasers generating ns- and ps-pulses operated with passive or active Q-modulator. However, it became more and more clear that such non-linear and multi-parametric system as a laser could support self-effecting, self-modulating mode of operation without any external devices or internal elements. Starting from the time of the laser's invention, the theoretical models of laser operation include mode spectrum genesis. This is logically understandable, as the open Fabry-Perot cavity is one of the main components of the laser system. However, the picosecond or, moreover, femtosecond pulse generator has thousands and thousands of modes. Theoretical description of few modes is possible and can be used for analysis of laser operation. However, solving, for example, fifty thousand equations that describe all operating modes is a problem and the results could be very far from the reality.

The author of this chapter considers another approximation. The logic of this is as follows. The laser generation develops from luminescence radiation, which is de-facto, an optical noise. Let us analyze how this noise is being modified propagating through the gain medium after the laser threshold is achieved. At each moment of time, the spectral width and averaged power level determine the statistical properties of radiation. So, depending on laser parameters, the exceeding of the maximal, stochastically appeared optical spike over the next smaller one irradiated during a cavity round-trip period, could be found. At some

conditions, the multiple, small-amplitude spikes saturate the amplification of the gain medium and stop the in-cavity power accumulation. Only the highest spikes that are able to saturate the non-linear absorber continue growing.

Around the 1960s, the properties of noise in radio-band were very well investigated on the way of radio rangefinders development. This theory was applied to describe the mode-locking process. Some difference was just in mathematical description: in radio-band the measured value is amplitude (strength) of the electromagnetic wave, and in optics, the square of this value, namely, intensity (power) of light. This approximation can estimate statistical parameters of generation: probability of single-pulse formation on the round-trip cavity period, depending on gain media spectrum width, rate of gain increase, cavity length, output mirror reflectance, and other laser practical parameters.

In this chapter, one can find interesting concepts, theoretical models, and experimentally proven techniques that for different reasons were not revealed in public at the moment they were proposed and demonstrated. Two different laser systems will be discussed: 1) single-frequency laser that, at certain conditions, is capable of slow self-modulation initiated by thermal processes in the cavity; 2) multi-mirror laser that, at certain conditions, is capable of self-mode-locking and generation of ultrashort pulses without any modulator.

This chapter represents philosophy of creation of laser pulses of different gradations:

1. "Slow" pulses of second duration
2. Microsecond pulses in millisecond envelope
3. Nanoseconds: passive and active Q-modulation
4. Picoseconds: passive, active, and natural auto-mode-locking
5. Femtosecond lasers
6. Attosecond and Zeptosecond

For today, hundreds of books describing the laser operational modes, design, constructions, and technologies are available. The condensed description can be found in an open-access encyclopaedia by Dr. Rüdiger Paschotta [1]. In this chapter, we often refer to the encyclopaedia pages, which typically contain a wide list of publications, discussing specific area of research. This chapter focuses mainly on some specific laser regimes and theoretical concepts, which are not considered in traditional books and in on-line encyclopaedia, and can be useful for the design of simple, low power-consumption, and environmentally-stable systems.

2. "Slow" pulses of second's duration

First of all, the initial question should be answered: how to slowly modulate such a fast operating and sensitive system as a laser. In principle, this can be provided by slow "delicate" changes of the gain or losses (or both) in a stationary operated laser with narrow spectral band. Such modulation is very difficult to provide in case of a multi-mode laser because of mode competition process: if output power of one mode is decreased, the others immediately grow up. Hence, first of all, a single-frequency operation has to be provided.

Let us consider an example of specific single-frequency laser [2, 3] that is capable of providing cavity losses periodical self-modulating. This regime has been achieved in the diode-pumped single-frequency Nd:YVO$_4$, Nd:YAG, and Nd:YLF lasers with metallic thin-film (10nm) selector. The main idea of the absorbing thin film selector operation is the following. The metallic film, with thickness Δd significantly smaller than the standing wave period ($\Delta d < \lambda/100$), is placed in the linear cavity. If a thin film plane is adjusted to the node surface area of any mode, the losses for this mode become close to zero and single longitudinal mode starts to operate. A detailed description of the interferometer with an absorbing mirror can be found in [2, 3].
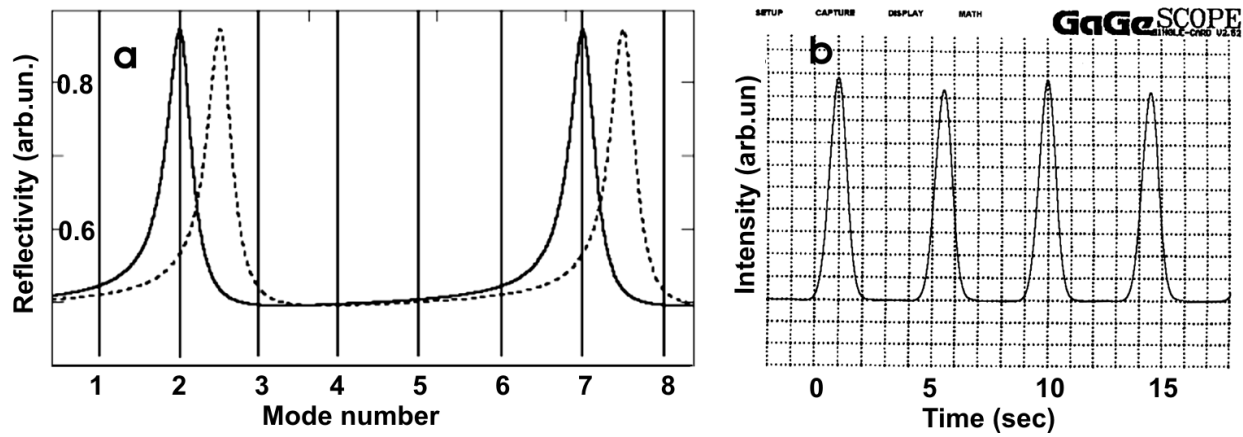
Figure 1. Mode switching mechanism: a) Vertical lines demonstrate laser cavity modes. The laser operates when the interferometer maxima (solid curve) coincide with the laser modes spectral positions, and does not – when the interferometer modes are located between the cavity modes (broken line); b) Oscillogram of the laser output power. One division of time scale is 1 sec. The peak power is approximately 0.5W. The radiation maxima correspond to the spectral positions of the interferometer maxima shown by the solid line in Figure 1a.

The pulses with duration of approximately 1 to 3 s and period of about 3 to 10 s (see Figure 1b), depending on pump power and thermo-optical properties of the cavity and gain crystal, have been observed. The effect has been explained by the thermal changes of the cavity length connected with the difference of the heat generation rate for operating and non-operating laser [4].

The self-pulsation regime of operation can be explained by periodical modulation of losses of a cavity with a thin-film selector caused by the thermally induced changes of optical length of an active medium. Let us assume that the thin-film selector is placed between the two nodes of neighbouring modes and the pump level is slightly below the threshold for both of the modes. At this moment, the laser does not operate; the maximum possible portion of pump power is transformed into heat and the temperature of the crystal increases. Because of the thermal elongation of active medium (and a total cavity), the positions of some nodes move to the absorbing thin-film location and the losses for this mode fall down. The mode switching mechanism is explained in Figure 1. Relative positions of the modes and the absorbing interferometer reflection peaks are shown. The interferometer is formed by a thin-film selector and an output coupler. The solid curve demonstrates resonance

position that provides laser operation. The laser starts to operate in the single-frequency regime. At maximum output power, the heat dissipation rate becomes minimal and crystal temperature starts decreasing. Further, the thin-film location "comes out" from the node position and interrupts the laser emission process (dashed curve in Figure 1a). After the laser action break-off, the temperature rises up again and the process repeats.

3. Microsecond pulses in millisecond envelop

The operation of a free-running laser can be described and understood in terms of gain-loss dynamics [5,6]. When a pumping source intensively irradiates the laser medium, the gain grows until it becomes equal to all losses. Starting from this moment, the number of newly "born" (generated) photons is greater than those "dying" (absorbed or scattered). The light intensity grows very fast (avalanche conditions) and the laser starts generating. Very soon, the stimulate emission becomes so strong that the pumping radiation cannot refill the inversion population - in other words, the gain drops down to the level when generation is interrupted. The laser pulse is finished and during the next generation pause the inversion population grows up again until the gain achieves the loss level and the next cycle of generation begins.

When counter-propagating narrow-bandwidth light waves are superimposed, they form a so-called standing-wave interference pattern, the period of which is half the wavelength [7]. This results in so-called spatial and spectral "hole-burning": a) in maxima of standing wave the inversion population is falling down, shaping periodical spatial grating of the gain along the active medium; b) the operating modes are "eating" the gain at their spectral positions and other modes start generating. These have various consequences for the operation of lasers:

1. Difficulties in achieving a single-frequency operation or operation with stable and repeatable parameters when generating in linear cavities;
2. The optical bandwidth and spectral structure of a free-running laser radiation is different when the gain medium is located in different resonator areas;
3. Spatial hole-burning can reduce the laser efficiency, when the excitation in the nodes cannot be utilized.

The ring cavities support running waves and spatial hole-burning can be eliminated.

4. Nanosecond pulses: Passive and active Q-modulation

The Q-switching is a technique which provides generation of laser pulses with extremely high peak power: MegaWatt to GigaWatt [5,8]. Here Q means a quality-factor of the laser cavity. Typical durations of such pulses are between several nanoseconds to few tens of nanoseconds. This effect is achieved by modulating the intracavity losses. Initially, the resonator losses are kept at such a high level that the laser cannot operate at that time. Then, the losses are suddenly reduced by modulator to a small value. So, the laser becomes highly "over-excited" and starts generating just after several flights of light along the cavity. When

the intracavity power has reached the value of the gain saturation, the laser radiation intensity drops down to the luminescence level. The resonator losses can be switched in different ways: through active and passive Q-switching.

For active Q switching, the losses are modulated with an active control element, typically either an acousto-optic or electro-optic modulator. Initially, there were also mechanical Q switches such as spinning mirrors or prisms. In any case, shorter cavities and more intensive pumping provide shorter lasing pulses.

For passive Q switching, the losses are automatically modulated with a saturable absorber. This can be a specific dye dissolved in liquid or solid matrix, some doped crystal or glass, and some bulk elements demonstrating the Kerr-type non-linearity. The pulse is formed as soon as the energy stored in the gain medium has reached a level sufficient to keep the absorbing particles in an excited state. The recovery time of a saturable absorber is ideally longer than the pulse duration. At this condition additional unnecessary energy losses would be avoided. However, the absorber should be fast enough to prevent the lasing when the gain recovers after the pulse termination.

5. Mode-locking

Mode-locking is a group of methods for laser generation of ultrashort pulses [9-13]. Typically, the pulse duration is roughly between 50 fs and 50 ps. To provide synchronous (phase-locked) operation of different modes, the laser cavity should contain either an active or a nonlinear passive element.

Figure 2 and Figure 3 demonstrate the difference between mode intensity and phase distributions for: (a) radiation that just is emitted at close to threshold conditions and (b) for already mode-locked radiation at the moment close to gain medium saturation. Simulation was done just for 10 modes to clearly illustrate the difference. In reality the number of operating modes may be tens or hundreds of thousands. The red line in Figure 2 shows the averaged mode intensity distribution. It is the same for any number of modes and any phase distributions. In any case, the initial gain medium luminescent radiation is a stochastic optical noise – a random sequence of occasionally irradiated spikes, which have different spectral content. The passive saturable absorber automatically selects (emphasizes) some spikes with relatively high energy and with relatively short duration. This results in some temporal uncertainty of the generation appearance and in generation of few ultrashort pulses on the cavity round-trip period because the gain medium continuously generates new noise patterns. The temporal distribution of radiation is "breathing" and is not ideally repeatable even on the neighbour round-trip periods of time. Moreover, the general view of time-intensity distribution of generation is unrepeatable from shot to shot – it could be one, or two, or even more high intensity pulses on the round-trip period.

In Figure 4 [14] two oscillograms of the laser output radiation are depicted: (a) an initial stage of generation development and (b) view of the mode-locked generation after non-linear absorber action. The arrows on the oscillogram (a) indicate the positions of strong

spikes (peaks are out of the picture) that were transformed later to the single ultrashort pulses. The oscillograms have been acquired with coaxial vacuum photodiode and analogue wide-band oscilloscope.
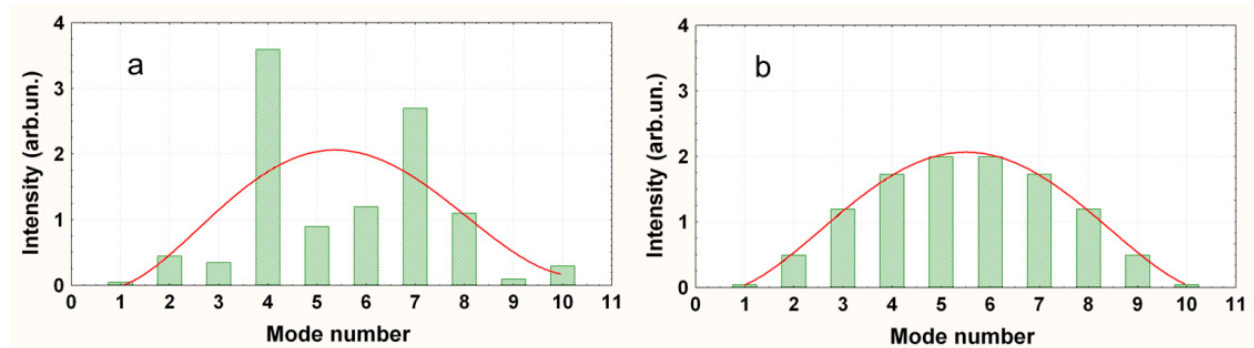

Figure 2. Spectral distribution of intensity of the modes: (a) at the beginning of generation development randomly modulated spectrum of a single noise patter; (b) at moment of pulse train emission. In both cases the red bell-shape line shows the averaged intensity distribution. Distribution (a) is chaotically being changed at each laser shot and during the generation development until achieves the distribution (b). The same is for the phases in Figure 3.
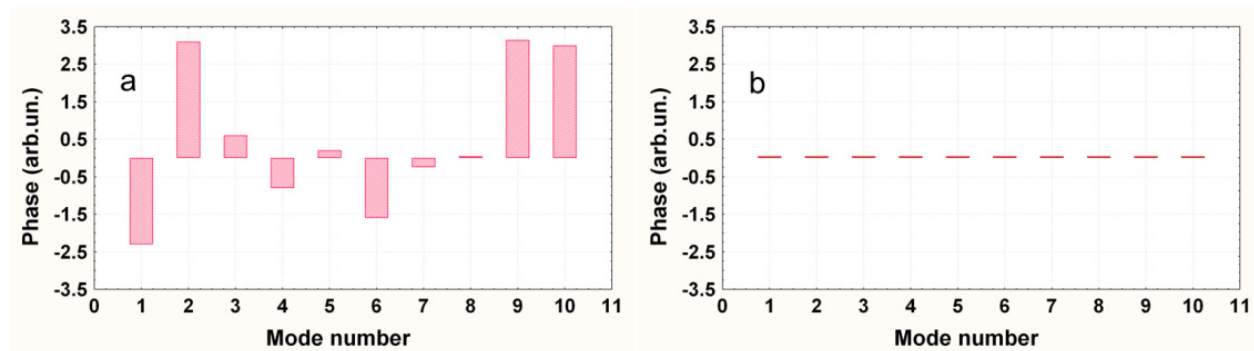
Figure 3. Spectral distribution of the phases of the modes: (a) at the beginning of generation development; (b) at moment of pulse train emission.

Each initial noise spike can be shaped by interference of the modes that belong to different parts of the spectrum and have different phase distribution. During the process of intracavity power increase even the neihbour (in time) spikes coud be modified differently. The ellipses in Figure 4 shows such case when only during two round trip periodes the first spike among three, initially being the smallest, became the highest.

In case of active modulation, the maximum of the modulator transparency very rarely coincides with occasional generated maximal spike of luminescence. However, since any spike is in-time repeatable on the round-trip period and, if coinciding with periodical maximal cavity Q-value, it will grow faster than even bigger spikes irradiated out of high Q-window. After hundreds of round-trips, this initially, maybe minimal pulse achieves the maximal amplitude and is generated as a train of laser pulses. Typically, at active modulation the pulse duration is longer but the jitter of the pulse appearance is much less as compare with passive modulation.
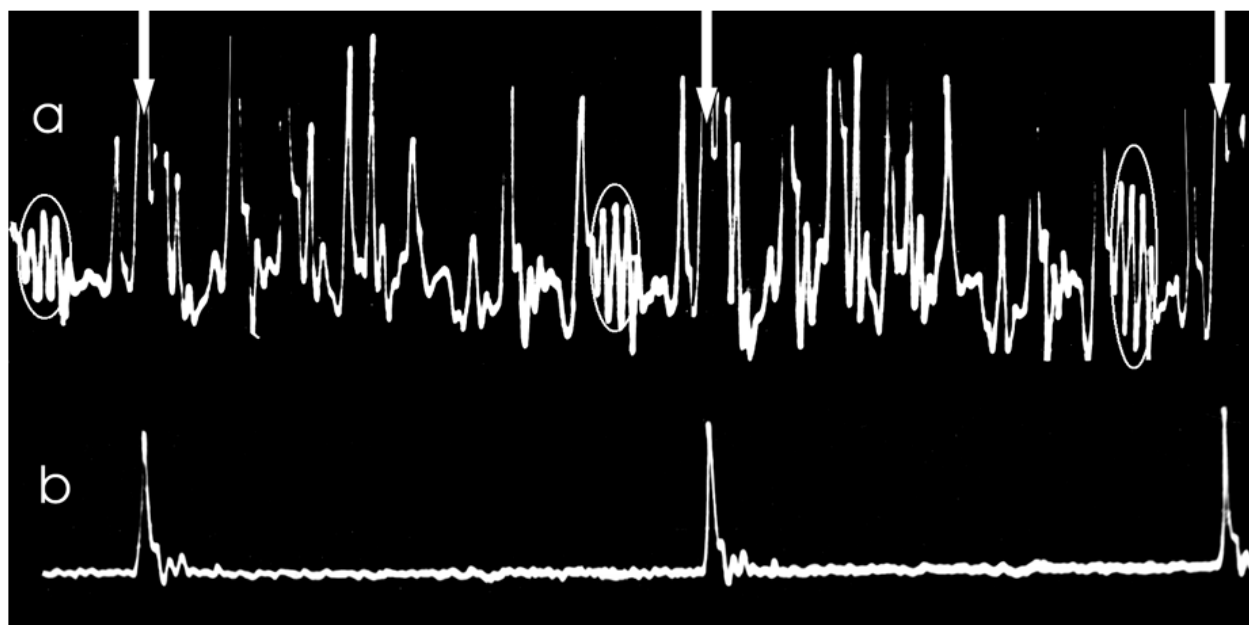
Figure 4. Oscillograms of the laser output radiation: (a) on the initial stage of generation development and (b) after non-linear absorber action. The arrows on the oscillogram (a) indicate the positions of strong spikes (their peaks are out of picture) that were transformed later to the single ultrashort pulses.

6. Propoperties of the optical noise

6.1. Mode formation and radiation dynamics

The phase and amplitude relations between the modes respond to the statistics of a normal (Gaussian) process. At the absence of phase modulation, a minimal possible duration of light random spike is inversely proportional to the total luminescence spectrum width. The amplification band typically has some specific intensity modulation. For relatively narrow spectral bands, the most energetic central modes introduce the main income into the pulse shape formation. At non-stationary pumping, the intensity and spectral width of the gain band is changeable in time that results in changes of random spikes statistics. Moreover, spectral content of the spikes additionally is being deformed because of dispersion, absorption and scattering processes in the cavity elements. As a result, the final time-intensity distribution may be absolutely different from the initial optical random noise distribution that was emitted at threshold conditions.

For the radiation propagating within the linear cavity of length L, the correlation function defers from zero, at least, on the time intervals $T_c = 2L/c$ (for the ring cavity $T_c = L/c$). The existence of signals correlation on T_c intervals means that the operational set of the modes is formed. At this moment, the averaged intensity of circulating in the cavity radiation should be significantly higher than the intensity of firstly irradiated luminescence pattern. After that moment, the temporal intensity distribution does not change significantly after each round-trip through the cavity. However, because of spectral dispersion of an amplification band and different spectral content of each spike, the intensity growth rate for each spike is different. During hundreds of cavity round-trips, the general view of a random noise-like

pattern (realization) changes and may be significantly reshaped by the moment of the final ultra-short pulses emission. The shortest spikes shaped during the total period of radiation development may be "late" and not have enough time to be "accelerated" to the maximum intensity. It means that the gain bandwidth may exceed the width, actually used at certain values of pumping, cavity length, material dispersion of the elements, and other laser parameters.

With a Fourier analysis, it is possible to transfer a signal from time domain to frequency and inversely. The mode-locking technology provides zero phase difference between all operational modes. At Gaussian shape of the operational spectral envelope, the pulse intensity has the same shape in time. If one modulates statically the spectrum (by interferometer, for example), the respective modulation appears in temporal intensity distribution. In case of the pulsed pumping, it is possible to modify the gain spectrum by variations of pump rate, cavity length, dispersion of the cavity elements, losses of the cavity to achieve finally different ultrashort pulse durations.

6.2. Statistical properties of optical noise

The theory of electro-magnetic noise was initially developed for the radio band. The main parameter considered in this range is electro-magnetic wave amplitude (E). In optics, because of very high optical signals carrying frequency, the intensity (I) that is a square of field amplitude (E) is considered and measured. Mathematical analysis of the optical stochastic signals with formal exchange E^2 to I has been done in [14]. For detailed description of the mode-locked process, let us repeat here this analysis with taking into account the parameters of the laser cavity. At the beginning, let us rewrite the formulas of random process theory [15] but in terms of intensity, instead of the amplitudes.

The famous Wigner's formula demonstrates the connection between autocorrelation function $k(\tau)$ (time domain) and spectral density $S(w)$ (spectral domain) [16]:

$$k(\tau) = \frac{1}{2\pi} \int_{-\infty}^{\infty} S(w) e^{jw\tau} dw, \tag{1}$$

$$S(w) = \int_{-\infty}^{\infty} k(\tau) e^{-jw\tau} d\tau. \tag{2}$$

The commonly used optical parameter Δf_e is an energetic spectral width of the random process:

$$\Delta f_e = \frac{1}{S_0} \int_{-\infty}^{\infty} S(w) \frac{dw}{2\pi}, \tag{3}$$

here $S_0 = S(w_0)$ is spectral density at maximum of spectral density distribution.

The luminescence field of a solid-state laser has a view of an optical noise with relatively narrow spectral width ($\Delta v / v \sim 10^{-1} \div 10^{-3}$). During evolution of the laser radiation on initial

stage (after the pumping applied), it becomes "more and more harmonical". The spectral width decreases for one to three orders of magnitude because of dispersion of the amplification coefficient [17].

The narrow band process is the stationary random process with a zero average value, the spectral density of which is concentrated near specific frequency f_0:

$$f_0 \gg \Delta f_e \tag{4}$$

A narrow-band stationary random process that has symmetrical spectral density with relation to f_0 is named a quasi-harmonic one. Luminescence bands of most laser ions are shaped by a superposition of several spectral lines, even in such homogeneously broaden system as, for example, Nd:YAG.

This results in important conclusions that typically are missed in books and papers:

- Typically, a wide gain band is not symmetrical relatively to the maximum and may have several local maxima. In principle, luminescence radiation of gain crystal is not quasi-harmonic signal. However, it transforms to one because of significant narrowing during generation evolution.
- Zeros of the dispersion curves do not coincide with intensity maxima. Non-monotonic dispersion curve (within the operational spectrum band) stimulates compression or extraction of the equidistant mode spectrum. This means the variations of round-trip time (for different frequencies), and, automatically, the extraction of the single ultrashort pulse duration.

The correlation function of the narrow band random process may be represented as:

$$k(\tau) = \sigma^2 \rho(\tau) \cos\left[w_0\tau + \gamma(\tau)\right], \tag{5}$$

here σ^2 is a dispersion of the process, $\rho(\tau)$ and $\gamma(\tau)$ are slowly modified functions as compare with $\cos(w_0\tau)$, $\rho(0) = 1$ and $\gamma(0) = 0$.

Correlation function of the wide band process typically is represented as:

$$k(\tau) = \sigma^2 \rho(\tau), \tag{6}$$

here $\rho(\tau)$ is normalized correlation function. As it follows from (1) - (6):

$$\sigma^2 = \frac{1}{2\pi} \int_{-\infty}^{\infty} S(w)\,dw = \bar{I} \tag{7}$$

Evidently, the parameter σ^2 represents total power of radiation and may be used for the normalization of the amplitudes or intensities of the random spike process. From a general view of the formula, describing probability density for the set of random values ξ_n [15], it is easy to get an expression for electromagnetic wave density distribution with substitution $n = 1$.

$$w_1(\xi_1) = \frac{1}{\sigma_1\sqrt{2\pi}}\exp\left[-\frac{(\xi_1 - m_1)^2}{2\sigma_1{}^2}\right]. \tag{8}$$

For the alternative electromagnetic field, the average value $m = 0$, and the final expression for the function, describing a density of probability of the amplitude A for the output laser radiation with an average intensity value of $\overline{I}$, is:

$$W(A) = \frac{A}{\sqrt{\overline{I}}}\exp(-A^2 / 2\overline{I}) \tag{9}$$

At that, the phase is distributed homogeneously on the interval $-\pi \le \phi \le \pi$.

6.3. Statistics of the laser optical noise pattern

From the statistics point of view, the different stages of the generation evolution may be classified as:

1. Luminescent field below the threshold: wideband random optical field;
2. First part of "linear" generation development (mode formation period): summarizing of the wideband and narrowband random signals;
3. Second part of "linear" generation development: quasi harmonic quasi periodical signal formation;
4. Nonlinear stage – gain or losses saturation.

Respectively, the statistical properties of radiation are different on each stage of generation genesis. By manipulating the initial internal radiation and laser external parameters, it is possible to achieve different results in the end of the path.

The sum of harmonic and quasi-harmonic signals [15] may be represented as follows:

$$S(t)+\xi(t) = A_m \cos(w_0 t+\varphi_0) + A_c(t)\cos w_0 t - A_s(t)\sin w_0 t = V(t)\cos[w_0 t+\psi(t)] , \tag{10}$$

here $A_c(t) = V(t)\cos\psi(t) - A_m\cos\varphi_0$, $A_s(t) = V(t)\sin\psi(t) - A_m\sin\varphi_0$.

A random function $V(t) > 0$ is envelope, and a function $\psi(t)$ is a random phase of the sum of harmonic signal and quasi-harmonic noise. From (10) it is easy to achieve:

$$V(t) = \{[A_c(t) + A_m\cos\varphi_0]^2 + [A_s(t) + A_m\sin\varphi_0]^2\}^{1/2}\ V(t) > 0, \tag{11}$$

$$\psi(t) = arctg\,\frac{A_s(t) + A_m\sin\phi_0}{A_c(t) + A_m\cos\phi_0}, -\pi \le \psi(t) \le \pi. \tag{12}$$

Envelope $V(t)$ and random phase $\psi(t)$ have one-dimension probability densities:

$$W(\upsilon) = \upsilon\exp\left(-\frac{a^2 + \upsilon^2}{2}\right)I_0(a\upsilon),\ \ \upsilon = V / \sigma, \tag{13}$$

$$W(\psi) = \frac{1}{2\pi}\exp\left(-\frac{a^2}{2}\right)\left\{1 + \sqrt{2\pi}a\cos(\psi - \phi_0)\Phi\left[a\cos(\psi - \phi_0)\right]\exp\left[\frac{a^2\cos^2(\psi - \phi_0)}{2}\right]\right\}, \quad (14)$$

here $a = A_m/\sigma$ is signal to noise ratio, $I_0(z)$ is Bessel function of zero's order with imaginary argument.

$$I_0(av) = \frac{1}{2\pi}\int_{-\pi}^{\pi}\exp\left[\pm iav\cos(\psi)\right]d\psi \quad (15)$$

$$\Phi(z) = \frac{1}{2\pi}\int_{-\infty}^{z}\exp\left(-\frac{x^2}{2}\right)dx \text{ is a probability integral} \quad (16)$$

From a general consideration, it is clear that the higher the average radiation power, the higher the number of random spikes amplitude variants that can be realized. Increasing the width of the probability density curve means that the probability of generation of two spikes with the close amplitudes increases versus time. This is an undesirable effect, because the closer the amplitudes are, the more difficult separating them and suppressing lower spikes on the non-linear stage of generation development becomes. To achieve complete mode-locking, it is necessary to maximize the difference between the amplitudes of the random spikes that makes the single pulse separation on the round-trip period of the cavity easier.

In [15], it has been shown that to calculate the number of excesses over certain curve C, it is necessary to estimate the joint density of probability for the envelope and for the derivative of this function. The final formula for the average number of positive excesses of the envelope $V(t)$ of the sum of random (noise) and quasi harmonic processes in unit of time is:

$$N_1^+(C) = \sqrt{\frac{-\rho_0''}{2\pi}}W = \sqrt{\frac{-\rho_0''}{2\pi}}\frac{C}{\sigma}\exp\left[-\frac{a^2}{2} - \frac{C^2}{2\sigma^2}\right]I_0\left(\frac{aC}{\sigma}\right). \quad (17)$$

Respectively, for the quasi-harmonic signal ($a = 0$) the view for (17) may be simplified:

$$n_1^+(C) = \sqrt{\frac{-\rho_0''}{2\pi}}\frac{C}{\sigma}\exp\left[-\frac{C^2}{2\sigma^2}\right]. \quad (18)$$

It is known that the square of the energetic width of the signal spectrum is proportional to the second derivative from the correlation coefficient. For the Gaussian spectral density function, taking into account (6), (7) it is possible to write:

$$\sqrt{\frac{-\rho_0''}{2\pi}} = \Delta f_e. \quad (19)$$

Thus, for quasi-harmonic optical signal that is correlated on time T_C (round-trip period), the average number of the intensity spikes that surely exceed the average radiation intensity level $\bar{I}$ may be found from the following:

$$n^+ = T_C \Delta f_e W\left(\frac{I}{\sqrt{\bar{I}}}\right) \tag{20}$$

Versus the generation development, the value Δf_e decreases, but $\sqrt{\bar{I}}$ increases. Thus, temporal dependence of n^+ depends on the functions mentioned above and might have complicated non-monotonous behaviour. Formula (20) demonstrates that spectral width and total radiation power determine all properties (statistics) of the laser radiation noise pattern. Hence, calculating these values at any moment of generation development, one can evaluate the statistical parameters of radiation.

6.4. Statistical properties of radiation on the "linear" stage of the generation development

In [18-20], the process of mode-locking in solid-state lasers has been analysed. It was shown that at the end of the linear stage, the noise pattern is a superposition of a great number of patterns emitted after the threshold conditions have been achieved. For increase of the output parameters repeatability, it was proposed to decrease a total number of the operating modes but with keeping the same a total spectrum width. Such mode number thinning out results in increase of repetition rate of the pulses and improves the pulses parameters repeatability. To check these dependencies, a Nd:glass laser with round-trip period in range 20 ps - 20 ns has been built and studied experimentally.

Starting from (9) and (20) with n =1, 2, one can find two maximal amplitudes C_1 i C_2 (the first and the second) probably generated on the laser cavity round-trip period. Typically, for small relative difference $\Delta = (C_1 - C_2)/C_1$ <<1 and for significant number of spikes $q = f_e T_C$ >>1, amplitude difference may be estimated as:

$$\Delta = \ln 2 / 2[1 + \sqrt{2\ln q} / (2\ln q - 1)]\ln q. \tag{21}$$

Spontaneous luminescence of a gain laser medium starts practically at the same moment with pumping. If the gain medium is located in the optical cavity, its emission may be separated on the portions equal to the light round-trip time between the cavity mirrors. Each of these patterns is independent noise realization. The total field at the end of the linear stage is the superposition of a great number of such patterns. Because of the amplification coefficient spectral dispersion, the initial spectral-temporal distribution deforms even on, so called, "linear" stage. It is clear that this classical term cannot be applied to the generation evolution period, which is characterized by signal frequency transformations.

Let suppose that an averaged in time envelope of the spectral intensity distribution is Gaussian: $I(w) = I_0 exp(-\Delta w^2/\delta)$. Total power after N round-trips of light is an integral through the spectrum with taking into account the growth of amplification coefficient. After each round-trip, a "fresh" noise pattern is added to the previous amplified radiation pattern. However, for a new noise realization, amplification exceeds losses in wider and wider spectral range. Because of these small differences in starting conditions, the summarized

radiation becomes non-Gaussian, even if each realization is Gaussian (but with different spectral width!). The function that describes average intensity change is the following:

$$\sigma_m{}^2 = \sigma_0{}^2 \exp\{\beta T_p (N-m)(N-m+1)/2\} / \sqrt{1+\alpha_0(N-m)}, \tag{22}$$

here $\sigma_0{}^2$ is average luminescence power, β is amplification coefficient growth rate; T_C is axial period of the cavity; N is number of round-trips from the moment of threshold completion for the central frequency; m is number of round-trips from the moment of the threshold up to m-th noise realization emission, α_0 is linear initial losses (dimensionless). Spectral width of m-th noise realization changes respectively:

$$\delta_m = \delta_0 \left[1+\alpha_0(N-m)\right]^{-1/2}, \tag{23}$$

where δ_0 is width of the luminescence of the gain medium. Formula (23) was acquired in assuption $\beta T_C N_{lin} \ll \alpha_0$, N_{lin} is a number of round-trips during total linear stage. Average intensity of final field accumulated in the cavity in the end of linear stage is as following:

$$\sigma^2 = \sigma_0{}^2 \exp\left[\beta T_C \frac{N_{lin}(N_{lin}+1)}{2}\right] \sum_{m=0}^{N_{lin}} \frac{\exp\left[-\beta T_C \frac{m(m+1)}{2}\right]}{\sqrt{1+\alpha_0(N_{lin}-m)}}. \tag{24}$$

It follows from (24) that the noise realizations with the numbers from $m = 0$ to

$$M=[2/\beta T_C]^{1/2}, \tag{25}$$

introduce the main income into the average intensity. They dictate the spectral parameters of the final field. For the typical laser parameters $\beta = 10^3 s^{-1}$, $T_C = 10^{-8}s$ one can estimate $M \approx 450$. Because of (23) the spectrum is not exactly Gaussian. However, difference in first actual M realizations is not significant, because usually $M \ll N_{lin}$.

Taking into account that on the "linear" stage, until there is no gain medium saturation, each realization develops independently, the final field may be considered as quasi harmonic random process with an average intensity:

$$\sigma^2 = \frac{\sigma_0{}^2 M}{\sqrt{1+\alpha_0 N_{lin}}} \exp\left[\beta T_C \frac{N_{lin}(N_{lin}+1)}{2}\right] \tag{26}$$

and the spectrum width

$$\delta = \delta_0 / \sqrt{1+\alpha_0 N_{lin}}. \tag{27}$$

Thus, the field formed up to the "linear" stage end is described by the statistics of quasi-harmonic random process. However, its evolution time is shorter as compared with classical estimations because of storage of energy by adding a significant number of optical noise realizations. It means that the spectral width is higher and the amplitude difference between

maximal spike and the second one is less than that predicted in linear model. As a result, the final probability of complete mode-locking is much less than it was estimated before. For different gain media, activator doping concentrations, methods of pumping, and levels of losses into a cavity, the linear stage duration is different. Hence, in certain limits the final spectrum width is not proportional to the starting (luminescent) width when different systems are compared. Though, affecting some parameters of the laser system, it is possible to satisfy requirements, providing the guaranteed achievement of single pulse generation on the cavity round-trip period.

6.5. Spectral-temporal dynamics

The noise pattern spectrum envelope only in average is proportional to the gain profile. In each specific "shot" the number of quanta in each certain mode may significantly differ from the statistically averaged value. Initial mode phases are distributed homogeneously in the range $-\pi \leq \varphi \leq \pi$. Mode-locking process results in two actions: introducing certain constant phase relations between the modes and in transferring the energy between the randomly modulated modes, so the spectrum envelope becomes smooth without chaotic intensity modulation.

Let us write the modes oscillations in specific point of cavity as the series:

$$A*(w,t) = A_0\sin(w_0t + \varphi_0) + A_1\sin(w_1t + \varphi_1) + \\ A_{-1}\sin(w_{-1}t + \varphi_{-1}) + \ldots + A_n\sin(w_nt + \varphi_n) + A_{-n}\sin(w_{-n}t + \varphi_{-n}) \tag{28}$$

here $w_{\pm n} = w_0 \pm \Delta w \cdot n$, w_0 is the central (maximal) frequency of the operational spectrum, $\Delta w = c/2L$ is an intermode frequency space, n is the mode number starting from the central one.
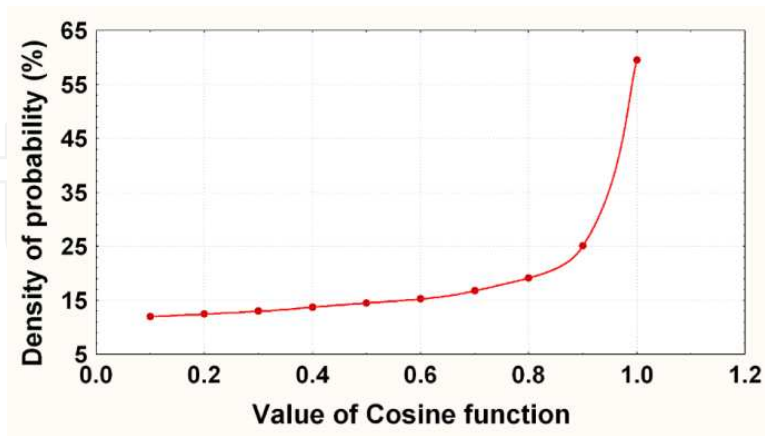
Figure 5. Probability to find a value of $cos(\varphi)$ function in intervals $0 - 0.1$, $0.1 - 0.2$,…$0.9 - 1$ at φ homogeneously distributed on the interval $-\pi/2 < \varphi < \pi/2$.

If the initial phase φ_n is not equal to zero, $\sin(w_nt + \varphi_n)$ may be represented as a series with the components: $A_c\sin(w_nt) + A_s\cos(w_nt)$, where $A_c = \cos\varphi_n$ and $A_s = \sin\varphi_n$ are the random values that changes slowly, as comparing with $\cos(wt)$. Let pay attention to the fact, that even in

case when a random phase is distributed homogeneously on the range $-\pi \leq \varphi \leq \pi$, the distribution density of A_c or A_s relate to cosine or sinus functions; in other words, this is not a homogeneously distributed function any more on the range of existence ($-1 \leq A \leq 1$). The probability to find a function on specific interval of meanings is inversely proportional to the rate of function changes, or to the derivative. For the function $A_c = \cos\varphi$ density of probability to find meaning into the interval $1 < A < -1$ is proportional to $\sin\varphi$. Thus, the most probable meaning for A_c is 1 in the interval $-\pi/2 < \varphi < \pi/2$ and -1 in the intervals $\pi/2 < \varphi < 3\pi/2$. For A_s the probable meaning in these intervals is close to zero. Figure 5 shows that in 58% attempts with phase distributed inside the range $-\pi/2 < \varphi < \pi/2$, the meaning of $cos(\varphi)$ function is inside the range 0.9-1. Respectively, interval 0.8-1 involves about 85% of all noise realization. The joint probability that two neighbour modes are generated with close phase values within this range is 0.72. At small number of operating modes in most number of the laser shots the sum $\sum\limits_{n} \sin(w_n t + \phi_n)$ may be exchanged to the $\sum\limits_{n} \sin(w_n t)$.
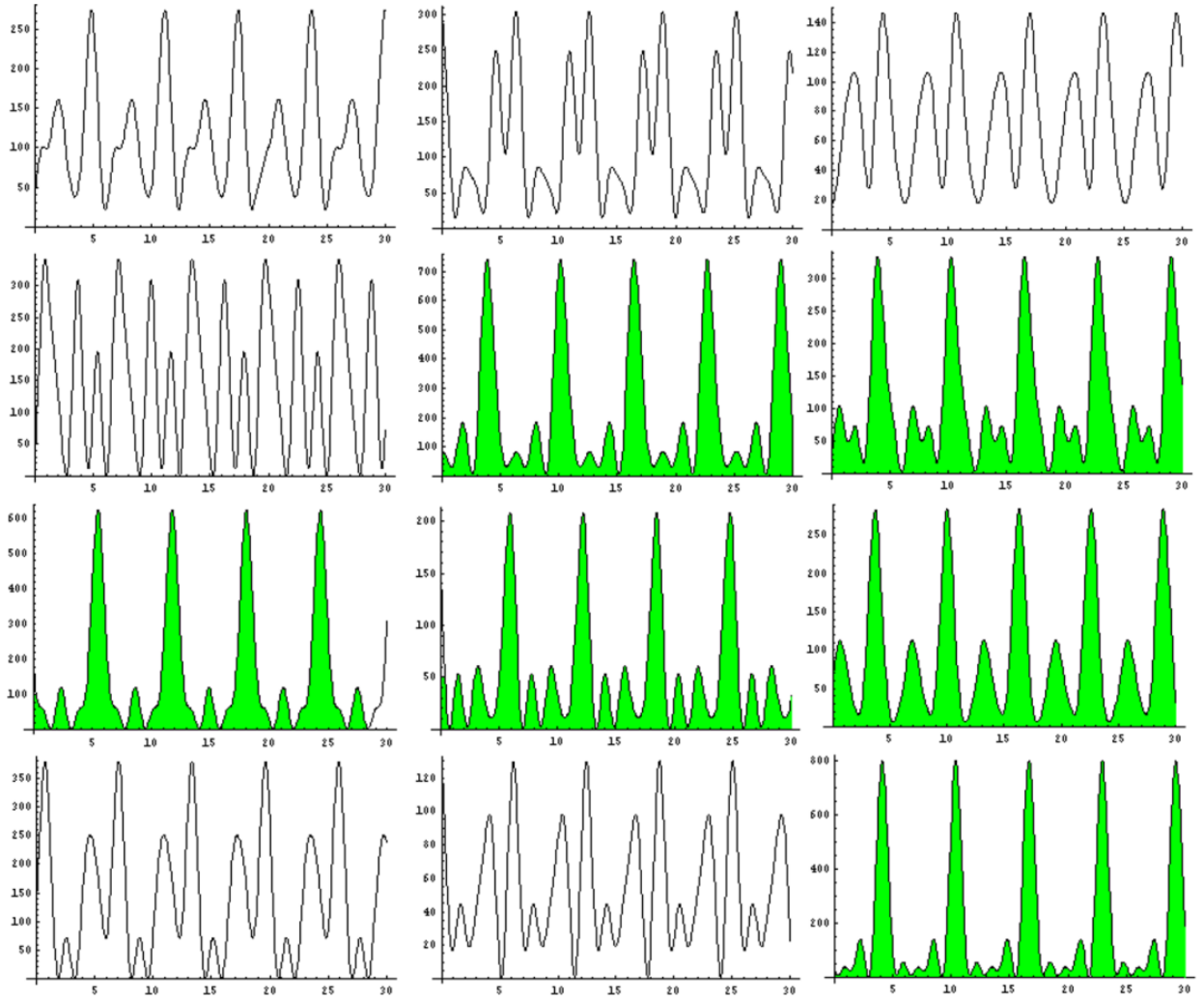
Figure 6. Computer simulation of the five mode interference (natural mode-locking process). Green oscillograms show the cases when the main peak contains above 80% energy of all pulses located on the round-trip period.

Figure 6 demonstrates a computer simulation of natural "mode-locking". The program generates random phases and amplitudes of five modes. Evidently, that half of the oscillograms contains 80% of round-trip period energy in a single pulse. This demonstrates "natural" mode-locking process, achieved without any non-linear elements placed into the cavity. Even with a weak non-linearity, such surely separated spike amplitudes may be easy additionally emphasized. However, there are more modes – less probability to generate "fully synchronized" spectrum. The solution is to keep a wide total spectral width but to decrease a total mode number. This can be done with low quality interferometer that does disturb the equidistant mode spectrum.

Moreover, in a real laser, the mode behaviour is not independent, especially if the amplification band is relatively narrow. Because of inversion hole-burning [7], two neighbour modes have maximal amplification because they are not overlapping in the centre of cavity where typically the gain medium is located. However, the next pair of the modes is overlapping with the first pair in the centre and near the mirrors. For the next 5th and 6th modes the amplification drops down because of spectral envelope's bell-like shape. Because of this phenomenon, practically anytime the laser output from the "pure" cavity (without selection) demonstrates modulation with axial period, which is a beating of two central high power modes. Taking into account the high probability that a "phase coefficients" A_c would be close to 1, one can understand why in big number of laser shots the emission demonstrates periodical structure, even without of any modulators or nonlinear elements.

6.6. Optimal spectral width of the ps-laser

It is well known that the wider the gain spectrum is, the shorter the pulses that can be generated are. However, some experiments have shown that this is not always true. This and the following sections analyse how the index of refraction and gain dispersions influence the duration of the spikes on the "linear" stage of generation evolution. The basic question is: what set of parameters provides the minimal duration of pulses before the non-linearity of the absorber or gain medium starts working.

In principle, the luminescence band of glass lasers has a sufficient width to generate femtosecond pulses. However, some effects result in an increase of the initial spike duration in the process of amplification and generation. First of all, because of the spectral dispersion of the amplification coefficient, the typical spike duration increases approximately 50 times [17]. To avoid this phenomenon, in [21], the interferometer was located in the cavity. It was aligned so that it flattened the maximum of the amplification band. The shortening of the pulses was about 1.5 to 2 times. However, it was much less than expected.

The next reason that makes it difficult to achieve short pulses in solid-state laser hosts is the dispersion of the material refractive index that results in broadening of the ultrafast pulses. At the conditions of low amplification near the threshold, the initial amplitude of the random short and intensive spike decreases during several round-trips through the cavity.

For the initially shorter pulses, the time of spike intensity development up to the absorber saturation energy is longer than for the relatively long pulses. Certainly, longer pulses survive in the process of generation evolution. Let us analyse the random spike spectrum genesis by taking into account amplitude-frequency transformations along the linear stage period.

To simplify the calculations, we assume that the spike spectrum shape is Gaussian, with an energy normalized to one. To study the process, we apply the Fourier transformation and follow all spectrum components developing.

$$I(t) = \frac{\delta}{\sqrt{\pi}} \exp(-\delta^2 t^2) = V(t)V^*(t), \tag{29}$$

Here δ is a luminescence spectrum width (dimension of δ is [s^{-1}]).

$$V(t) = \frac{1}{\sqrt{2\pi}} \int_{-\infty}^{\infty} \{\frac{\exp[-\frac{w-w_0}{\delta}]^2}{\delta\sqrt{\pi}} \exp[\beta T_C \frac{N(N+1)}{2} - N\alpha_0(\frac{w-w_0}{\delta})^2]\}^{1/2} \exp(-i\Delta\Phi)\exp(-iwt)dw \tag{30}$$

The first exponent in (30) describes the amplitude distribution of the spectral components of a pulse with maximum at w_0, the second one shows the amplification depending on the number N of the light field round-trips with the axial period T_C, initial (linear) coefficient of the losses α_0, and amplification coefficient increase rate β. An expression for the phase modification is as following:

$$\Delta\Phi = \frac{2\pi\Delta nL}{\lambda} = \frac{dn}{dw}|w-w_0|wT_qN, \tag{31}$$

here Δn is refractive index changes (at tuning out of w_0); L is a total length of the gain media passed by the light during the whole linear stage of generation; dn/dw is the refractive index dispersion; T_q is time of a light single pass through the gain medium.

Let us consider, at first, the pulse evolution that is represented by (29) – (31). The final expression for the single pulse intensity is as following:
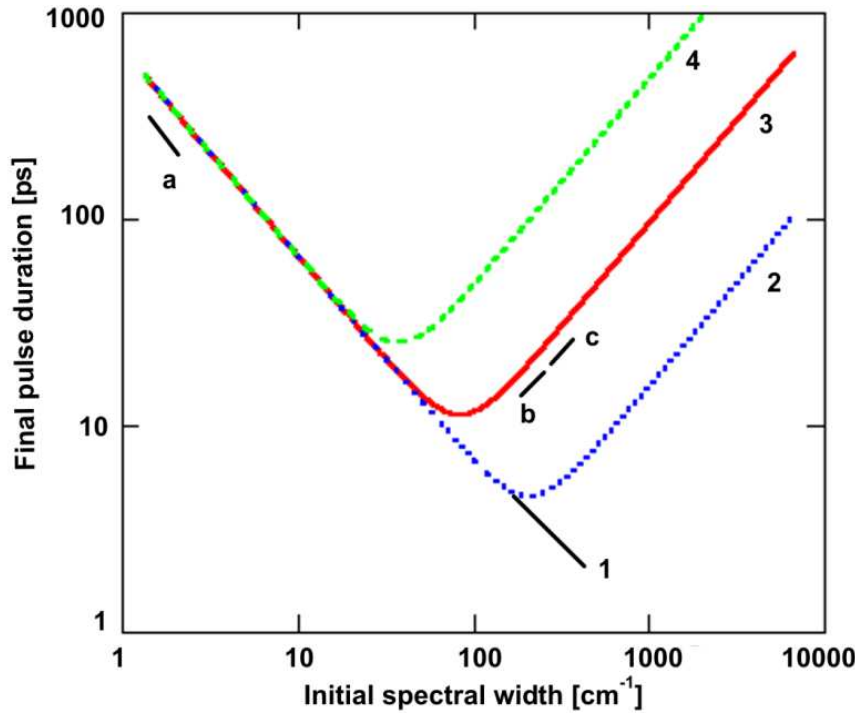
$$I(t) = \exp[\beta T_C \frac{(N+1)N}{2} - \frac{\Delta(aw_0+t)^2}{2(\Delta^2+a^2)}][2\delta\sqrt{\pi(\Delta^2+a^2)}]^{-1}, \tag{32}$$

here the designations are: $\Delta = \frac{1+\alpha_0 N}{2\delta^2}$, $a = \frac{dn}{dw}T_qN$.

From (32), it follows that the final inverse duration is connected with the initial one as:

$$\delta' = \delta[1+\alpha_0 N]^{1/2}[(1+\alpha_0 N)^2 + (2\delta^2 \frac{dn}{dw}T_qN)^2]^{-1/2}. \tag{33}$$

Figure 7. Dependence of the spike duration at the end of linear stage vs the initial noise pattern spectral width for different values of the refractive index dispersion $dn/dw = 0$ (1), $0.13·10^{-17}$s (2), $0.8·10^{-17}$s (3), $5·10^{-17}$s (4).

Figure 7 demonstrates the dependency of the pulse duration at the end of the linear stage Δt on the start spectrum width δ of the random spike at different values of the product $T_q(dn/dw)$. For $(dn/dw) \neq 0$, the curves coincide in the range of small δ meanings. For wide δ, the final Δt depends on the specific value of the product $T_q(dn/dw)$. In Figure 7, the letters mark the spectrum width for (a) Nd:YAG, (b) Nd:phosphate glass, (c) Nd:silicate glass.

At the end of the linear stage of generation, $N\alpha_0 >> 1$ and expression for the δ' may be simplified:

$$\delta' = \frac{\delta}{\sqrt{\alpha_0 N}} \text{ for the small } \delta; \tag{34}$$

$$\delta' = \frac{1}{\delta}\sqrt{\frac{\alpha_0}{N}}\left(2T_q\frac{dn}{dw}\right)^{-1} \text{ for the big } \delta. \tag{35}$$

From Figure 7, it is evident that the final spike duration Δt has a minimum. This area determines the certain start spectral width that, at some given set of the parameters (dn/dw, α_0, β, T_c, T_q), can provide the minimal duration of the spikes Δt_{min} at the end of the linear stage. From the (33) the conditions of the Δt_{min} achievement may be deduced:

$$2\delta^2\frac{dn}{dw}T_q = \alpha_0 \tag{36}$$

It follows from (36) that, for example, for the Nd:silicate glass (T_q =10^{-9} s, (dn/dw)= $8 \cdot 10^{-18}$ s) the optimal initial spectrum width is $\approx$ 70 cm^{-1} but the real one is about 250 cm^{-1}. Thus, to achieve minimal ultrashort pulses in the laser with Nd:silicate glass, it is necessary to narrow the initial luminescence spectrum width 3-4 times. The use of prisms is not appropriate in this case because with spectrum narrowing, it simultaneously results in the increase of the product $T_q(dn/dw)$. As an element with anomalous dispersion, an interferometer may be used. In this case, the etalon automatically plays the role of a gain spectral dispersion flattener.

By decreasing the losses (e.g., by improvement of cavity construction), the value Δt_{min} moves to the smaller spectral width values. If β stays the same, the relative amplification growth is higher in a system where α_0 is less. In this case, the spike spectrum width grows faster and natural spectrum selection process is restrained. If one decreases α_0 at relatively small initial spectrum Δ <30 cm^{-1}, the spike duration decreases because of the process of natural spectrum selection weakening. Inversely, for Δ >60 cm^{-1} the duration increases because of negative influence of the refractive index dispersion.

The starting losses α_0 include linear losses on cavity elements, on mirrors (output), and non-saturated losses in absorber. To achieve Δt_{min}, it is necessary to vary mirror reflection only, because decrease of the absorber density makes the pulse discrimination worse. For garnet type media, the highly reflecting mirrors are preferable; for glasses, it is better to use low reflecting mirrors.

Increase of the product βT_C (with the other parameters staying the same) results in Δt_{min} decrease. This phenomenon is connected with diminishing of the total number of the round-trips during the linear stage of the generation development. Having a low threshold and high amplification increase rate β, the garnets have lower located curves $\Delta t(\delta)$ as compared with glass hosts. This explains why these media, being with about two order of magnitude different luminescence bandwidth, demonstrate ps-pulses with durations just 3-5 times different. The phosphate glasses that have narrower luminescence bandwidth as compared with the silicate ones can provide shorter pulse generation. In all cases, possible variations of the laser parameters may minimize the random spike duration at the end of the linear stage of the generation development.

7. Experimental results

7.1. Spectrum modulation with dynamical interferometer

The mode-locking process supposes introducing of the certain amplitude-phase relations between all generating modes. In known techniques, phase locking is typically provided simultaneously along the whole actual spectral range. However, the condition of simultaneous phase regularization is not obligatory. In principle, the modes may be linked step by step, if a total mode number is relatively small or the time of generation development is relatively long [14]. In this case, the process of mode-locking spreads consequently from small group of modes to the whole spectrum. The simplest way to

build such a system is to install into a laser cavity an additional mirror with a piezo-driver. This three-mirror cavity is a dual-interferometer system. Let us place an interferometer with base length l_{0i} into the cavity with an optical length $L_C = kl_{i0}$, where k is integer. A diagram in Figure 8 shows the case where $k = 10$. Because of different cavity and interferometer lengths, there are k cavity modes located between two peaks of the interferometer. Internal mirror should be with low reflectivity and do not disturb significantly the mode spectrum of the main cavity. For two interferometers with bases of different optical length, the velocity of the reflection peak motion in the frequency domain is higher for the interferometer, which has shorter optical base. In principle, it is possible to move the interferometer peak from mode to mode position exactly during the light round-trip time along the cavity. In this case, relatively fast modulation with intermode beating frequency is realized by the relatively slowly moving mirror. This system can be named as an "optical lever" technology.
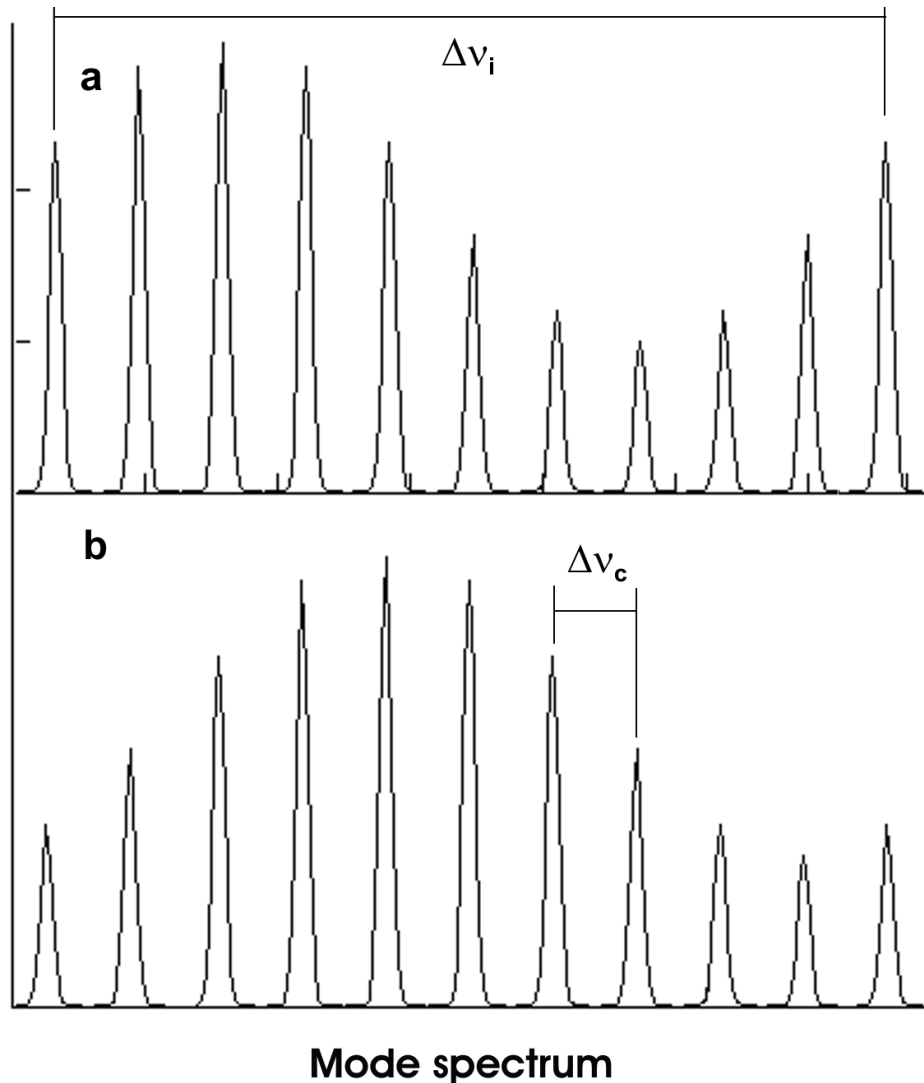
Mode spectrum

Figure 8. Examples of the mode spectrum fragments: (a) at time moment t and (b) at $t+2T_C$ – after two round-trip periods. Cavity length is equal to ten interferometer lengths: $L_C = 10l_i$. For illustration purpose the modulation depth is significantly increased.

To find the conditions of such mode-locking, let us suppose the optical length of the interferometer l_i changes with constant speed V. In this case, $l_i = l_{0i} + Vt$, here l_{0i} is the start interferometer length. The position of the n-th transparency maximum (of an unmovable interferometer) is described as:

$$v_n = 1/\lambda_n = n/2l_i, \text{ here } v = 2l_i/\lambda_{n0} \tag{37}$$

Differentiate (37) with respect to time and get n-th interferometer maximum frequency changes rate. With condition $Vt \ll l_{0i}$ (because $Vt \cong (1-10)\lambda_{n0}$, and $l_{0i} \cong 10^4\lambda_{n0}$) it is easy to achieve:

$$\frac{dv}{dt} = -\frac{nV}{2l_i^2} = -\frac{l_{i0}V}{\lambda_{n0}\left(l_{i0} + Vt\right)^2} \cong -\frac{V}{\lambda_{n0}l_{i0}}. \tag{38}$$

With the moving mirror the new cavity mode has the maximum quality consequently in each new T_c interval. Let us find such a mirror speed that provides the interferometer peak motion from the mode position to the next one for the time of the light round-trip in a linear cavity $T_c = 2L_c/c$:

$$\left(\frac{dv_n}{dt}\right)T_C = -\Delta v_C. \tag{39}$$
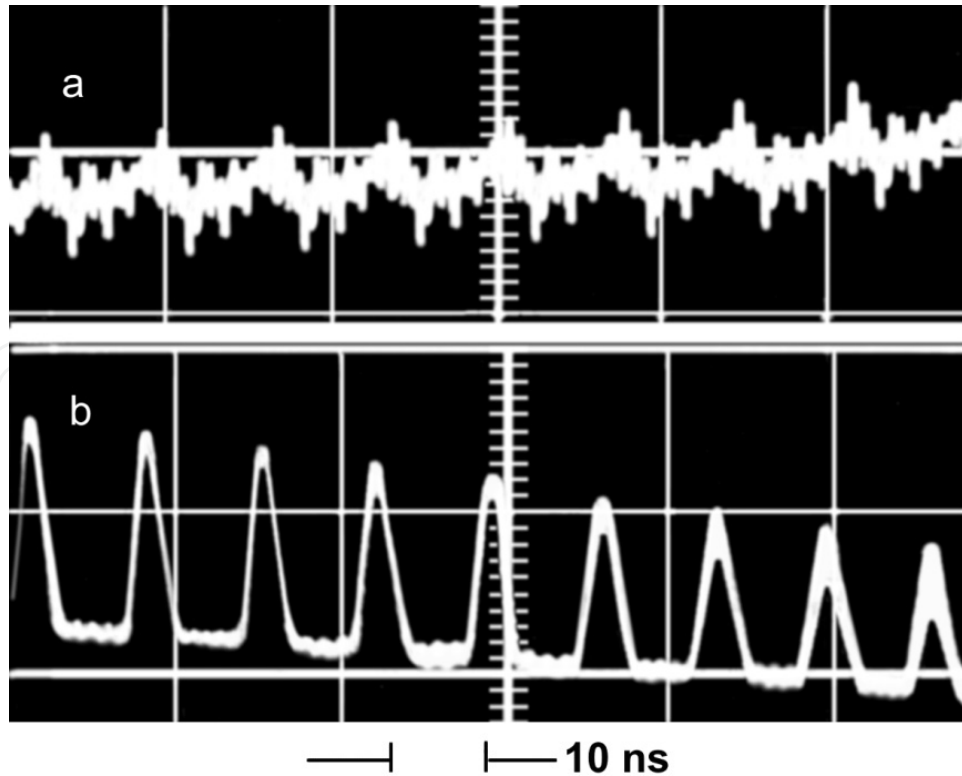
Figure 9. The oscillograms of laser output (a) with unmovable internal mirror and (b) with movable mirror.

After substitution into this equation dv/dt and T_C the value of V can be found. Intermode space Δv_i for the ring cavity is $\Delta v_i=1/l_i$, and for the linear one – $\Delta v_i=1/2l_i$. Introducing the coefficient $\gamma = 1/2$ for the linear cavity and $\gamma = 1$ for the ring one, finally the formula for the resonant mirror speed is:

$$V = \gamma\lambda_{n0}\Delta v_p^2 / \Delta v_i. \qquad (40)$$

Figure 9 demonstrates the oscillograms of the laser output (a) without interferometer and (b) with scanning interferometer. The interferometer mirror was moved by the piezo-transducer. Cavity length L_c was 200cm, interferometer base l_i was 0.25 cm that provided $k = 800$. With laser operational wavelength $\lambda = 1.06$ microns, the mirror velocity was about $V = 5$ cm/s. For lower k values the necessary mirror velocity should be higher. Hence, the mechanical motion of the mirror could be hardly achievable. In this case the electro-optical system should be used to control the cavity modes properly. An inclined interferometer limits the total spectrum width and the ultrashort pulses are not achievable with this technique. To solve this problem, the normally installed mirror should be used. To avoid back reflection that results in parasitic selection, a thin film selector should be used as a mirror. The properties of such a system have been described in section 2.

7.2. Laser with anti-mode-locking: "Black" pulses generation

Any periodical signal may be represented as a sum of harmonics with specific amplitude and phase coefficients. The scanning interferometer mirror may be moved with changeable velocity, following the special function. In this case, because of interference of the modes with certain combinations of the phase, the pulse shape may be specially designed [14].

One of the interesting examples of such laser generation is "anti-mode-locking". If the interferometer mirror is moved with the speed as doubled to the resonance one, the zero-phase difference is dictated to each second mode. The neighbour modes are modulated in anti-phase conditions. Figure 10 demonstrates several examples of simulated (left column) and experimentally generated (right column) pulse trains. The cavity length was 525 cm. That corresponds to a 35 ns round-trip time. The interferometer base was about 1.5 cm, with a resonance speed of about 4 cm/s.

Figure 10a – resonance mirror motion; it is classical mode-locking. Figure 10b – average mirror speed is two times higher as compare to the resonance one; motion is with acceleration. Figure 10c – motion with acceleration two times higher as in case (b). Figure 10d – average mirror speed is two times higher compared to the resonance one; even modes are in anti-phase conditions to the odd modes. ("anti-mode-locking"). The picture is inversed to the classical mode-locking (Figure 10a). On the background of the quasi-cw generation there are narrow peaks of radiation absence, or "black pulses".
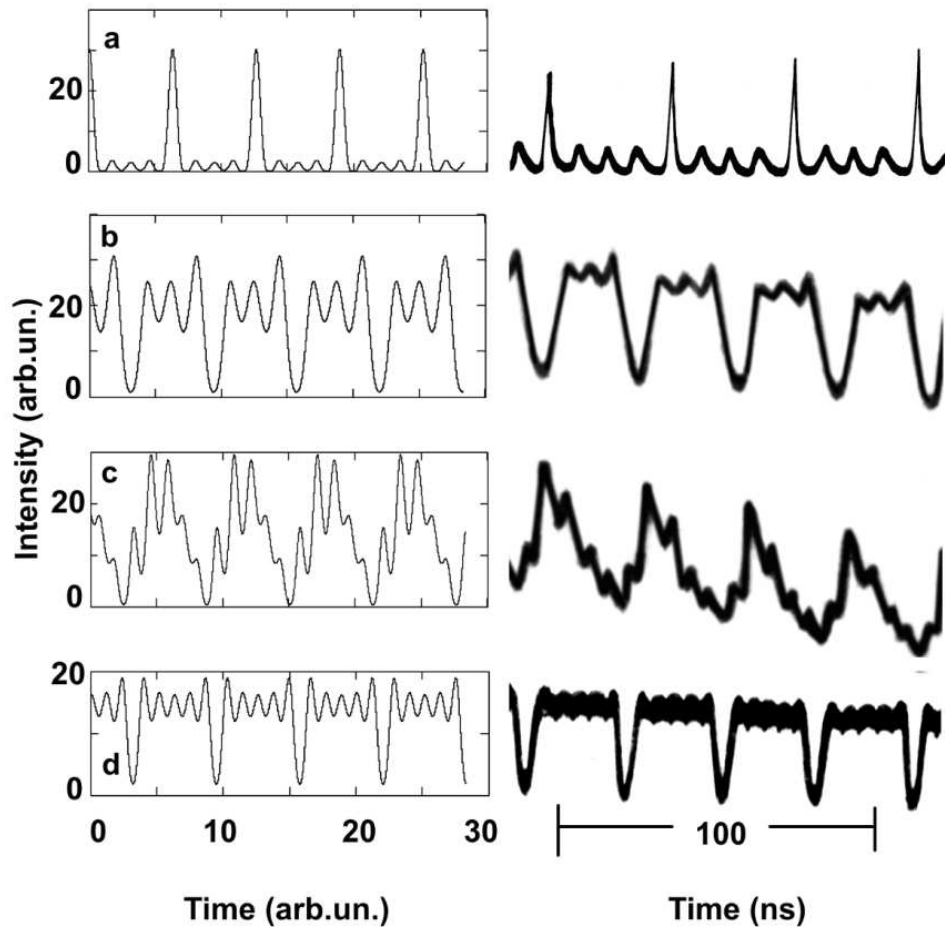
Figure 10. Simulated (left column) and experimental (right column) oscillograms in case of mode-locking (first row), anti-mode-locking (fourth row) and with some phase-shifted modes (second and third row).

7.3. High pulse repetition rates

In various applications such as telecommunications, pulse trains with multi-gigahertz pulse repetition rates are required. The resonators of the bulk lasers are usually too long to achieve such repetition rates with fundamental mode-locking. The high repetition rate pulse trains were obtained with harmonic mode locking [22, 23], when the active modulator worked at frequency multiply integer higher than the inverse cavity round-trip period. Similar research but at passive mode-locking has been provided in [24].

In this section, a 50-GHz repetition rate generation from the Nd:glass laser with 45-MHz cavity is described. The system was of modulator free [14]. This work was completed approximately nine years before the first self-starting Ti:sapphire laser was demonstrated. However, honestly saying, during Nd:glass laser's experiments, the role of the Kerr-type non-linearity was not understood.

The construction of the high repetition rate laser is very simple. The cavity contains just one additional low reflecting mirror that is installed so that the short base interferometer length (l) is exactly an integer multiple (n) of the full cavity length (L) (with heated gain medium): L

= *nl*. At this condition, the ultrashort pulse, running back-and-forth inside the interferometer, after *n* reflections, exactly coincides with the pulse that was running along the entire cavity. Since the total spectral width is the same, the pulse duration remains the same. The multiplication of ps-pulses results in periodical modulation of spectrum and, respectively, in a decrease of total mode number. At this condition, even without a non-linear absorber but with an aperture installed near the output mirror, the laser generated a train of ultrashort pulses. With a fourth mirror, which shapes a new interferometer with a base length integer to the first interferometer, the pulse repetition rate was increased again. Figure 10 demonstrates oscillograms of the mode-locked generation (a, c) and harmonic mode-locked (b, d). A photograph (e) shows the two-photon luminescence track achieved with a four-mirror cavity without a non-linear absorber. The pulse duration is 11±2 ps and the period of repetition is 20 ps. In all cases, the total cavity round-trip length was 6.6m (22ns).
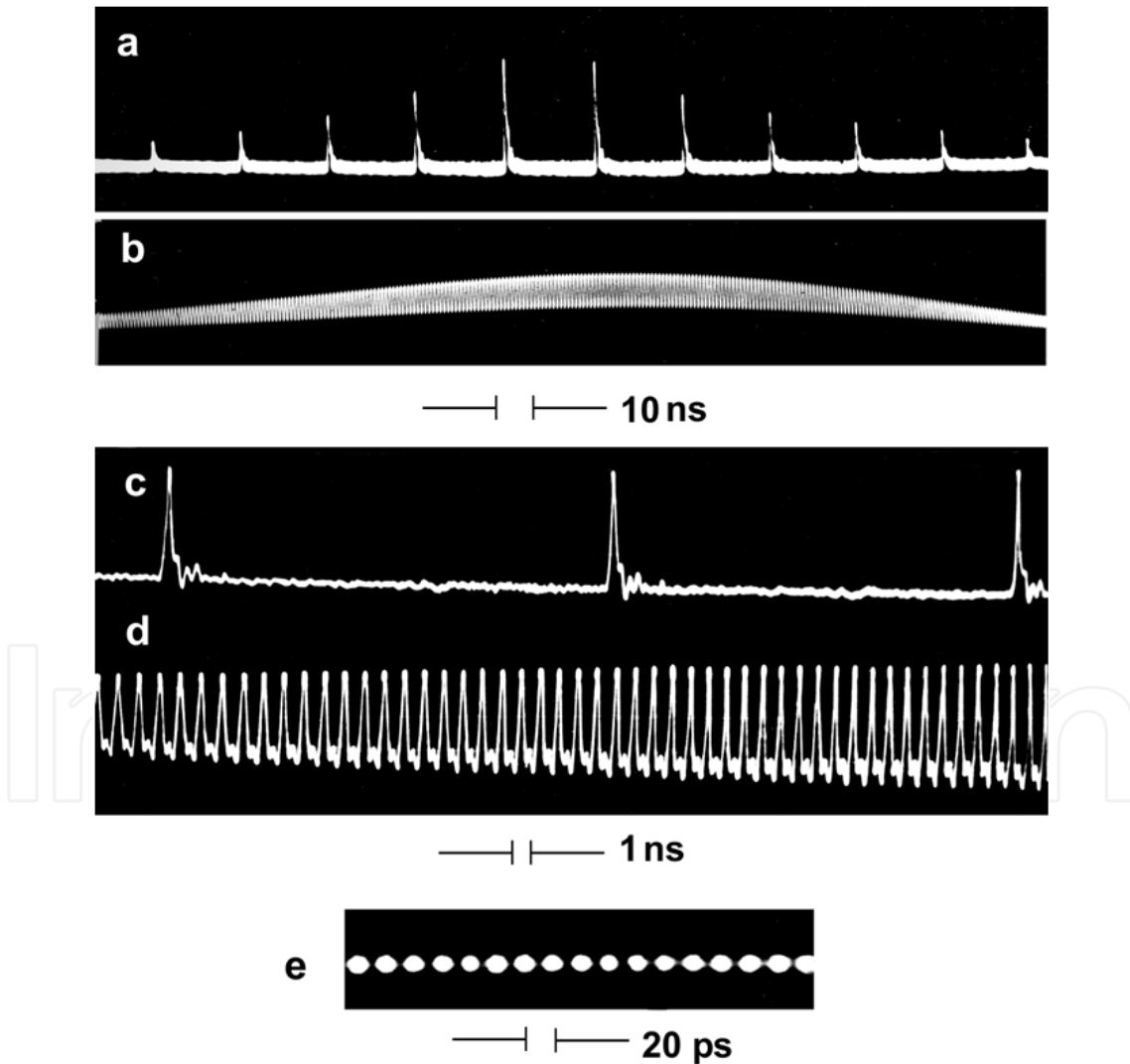
Figure 11. Oscillograms of the mode-locked generation: (a) total train; (c) three-pulse zoomed fragment. Three-mirror cavity: (b) total train; (d) zoomed fragment – period 0.98 ns. (e) Photo of two-photon luminescence track at four-mirror cavity – period 20 ps.

From my personal experiences, the idea to use an interferometer in the mode-locked laser cavity is typically rejected by project or paper reviewers because of supposed strong interferometer dispersion, which affects equidistant mode spectrum and makes short pulse generation impossible. In response, it should be specially emphasized that maximal exceeding of the gain over the losses in an free-running laser could be around 3-4%; hence, to shape the necessary spectral structure, the interferometer should provide about 5% modulation depth, which practically does not shift the modes. Moreover, it is possible to use the interferometer with absorbing mirror (see in section 2), which demonstrates a unique property – it does not reflect light at normal beam falling on the interferometer. In other words, there is no disturbance of the mode spectrum with such an interferometer.

8. Femtosecond pulses

From a theoretical point of view, the basic principles of picosecond and femtosecond pulses generation are the same [9-13]. The difference is in some parameter values. Femtosecond pulses have three orders of magnitude shorter duration than the picosecond ones. Hence, they require much wider operational spectral bands and faster mechanisms of modulation. Because of dispersion, the broadening of fs-pulses happens faster when propagating through the optical elements. Because of very high pulse peak power, the non-linear processes are routine problems for fs-lasers. Practically all types of ps-lasers were repeated in fs-lasers. They are bulk lasers with open cavity, fiber lasers, dye lasers, and semiconductor lasers. Disregarding the construction variety, principles of operation of all these systems are the same, or very similar. In the last five years, fiber lasers were the most dynamically developed segment of the fs-laser. The efforts of researchers are focused on suppression of non-linear effects, on increase of output average power, and on exploitation of new spectral ranges.

9. Attosecond and zeptosecond pulses on the way to yoctoseconds

The attosecond pulse generation and measurement are the hottest subjects of popular and solid scientific journals [25]. With achievement of this duration range, these super-ultra-short laser pulses became an instrument of intra-atomic process investigation. For the first time ever, researchers are capable of seeing how an electron "jumps" between atoms. The peak intensity of the as-pulses approaches and overcomes $10^{18}\,\mathrm{Wcm^{-2}}$. This is a powerful tool in studying the ultrafast phenomena, such as the chemical/biological transformations occurring on the femtosecond range of durations. An attosecond control of collective electron motion in plasmas has been provided in [26]. There are two ways to generate an attosecond pulse or pulse train [27]. One is through the nonlinear processes of the superposition of high order harmonics generated in the laser-gas atom interactions. The limitation is that the laser intensity should be low enough to avoid the ionization of atoms. Typically, the efficiency of harmonic emission from the atoms is low. The other way is to generate high order harmonics from the dense surface of plasma created by the high-

intensity femtosecond laser. Till now, 12 attoseconds is the world record for shortest controllable time [28].

The femtosecond lasers are more and more used as the sources in high energy atomic and nuclear investigations – see, for example [29]. It was shown that in the scattering of 100-fs laser pulse with an intensity of around 10^{19} W/cm^2 by a counter propagating electron with an initial energy of 10 MeV, a crescent-shaped pulse with pulse duration of 469 as and the photon energy ranging from 230 eV to 2.5 keV is generated in the backward direction. Recently the Internet brought us a new word: Yoctosecond – 10^{-24} seconds. The explanation what this is and where it could be used is very simple and fundamental: this is time taken for a quark to emit a gluon [30].

10. Conclusions and epilogue

1. Theory of random processes, initially developed for the radio-band frequencies, has been applied to describe the properties of the narrow-band optical noise and dynamics of the linear stage of generation evolution.
2. Theoretical analysis of the optical noise properties demonstrated high probability of the "natural mode-locking", when the main part of light energy accumulated in the cavity may be concentrated in a single pulse.
3. It has been shown that for each set of the solid-state laser parameters, there is a specific width of the amplification band that provides minimal duration of random spikes at the end of linear stage of generation. It was shown that two media, having, at least, one order of magnitude difference in luminescence spectrum width, might generate pulses of the same duration.
4. The harmonic mode-locked generation, achieved in a three-mirror cavity without a non-linear absorber, has been demonstrated in 22-ns cavity of Nd:glass laser.
5. A new method for controllable mode-locking with the help of "optical lever" – movable mirror placed into the laser cavity – has been proposed. The anti-mode-locking process with "black pulses" generation has been realized. Generation of rectangular and triangular ns-pulses has been achieved.

During the 50 years of their history, the pulsed lasers passed from seconds to zeptoseconds or about 20 orders of magnitude into the short duration's side. This road was not smooth and easy. Every time, starting from huge, complex, ineffective, and very expensive machines, the lasers became elegant, economical, more powerful and smart instruments in science, technology, medicine, and everyday life. We hope this chapter and this book will be useful for a wide spectrum of specialists, for professors and students, and for those who are interested in history and in future of the laser technologies.

Author details

Igor Peshko
Department of Physics and Computer Science, Wilfrid Laurier University, Canada

Acknowledgement

11. References

[1] Encyclopedia of Laser Physics and Technology.
http://www.rp-photonics.com/encyclopedia.html (accessed 6 May 2012).

[2] Jabczyński J, Firak J, Peshko I. Single-frequency, thin-film tuned, 0.6 W diode-pumped Nd:YVO$_4$ laser. Applied Optics 1997; 36(12) 2484-2490.

[3] Peshko I, Jabczyński J, Firak J. Tunable Single- and Double-Frequency Diode-Pumped Nd:YAG Laser. IEEE J QE 1997; 33(8) 1417-1423.

[4] Peshko I, Jabczynski J. Thermally induced pulsation in the solid-state single-frequency diode pumped laser. Optica Applicata 1999; XXIX (3) 319-325.

[5] Tang C, Statz H, de Mars G. Spectral output and spiking behavior of solid-state lasers. J. Appl. Phys. 1963; 34 2289-2295.

[6] Zvelto O, Principles of Lasers. Heidelberg: Springer; 2010.

[7] Encyclopedia of Laser Physics and Technology. Spatial Hole Burning.
http://www.rp-photonics.com/spatial_hole_burning.html (accessed 6 May 2012).

[8] Encyclopedia of Laser Physics and Technology. Nanosecond Lasers.
http://www.rp-photonics.com/nanosecond_lasers.html (accessed 6 May 2012).

[9] Rullière C. Femtosecond Laser Pulses: Principles and Experiments. New York, USA: Springer; 2005.

[10] Diels J.-C, Rudolph W. Ultrashort Laser Pulse Phenomena: Fundamentals, Techniques, and Applications on a Femtosecond Time Scale. Technology & Engineering. Elsevier Science Publishing Co Inc Academic Press Inc; 2006.

[11] Kärtner F.X. Few-Cycle Laser Pulse Generation and its Applications. Berlin: Springer; 2004.

[12] Topics in Applied Physics: Ultrashort Light pulses Picosecond Techniques and Applications Ed.S.L.Shapiro. Berlin, Heidelberg, New York Springer-Verlag 1977.

[13] Encyclopedia of Laser Physics and Technology. Mode locking. http://www.rp-photonics.com/mode_locking.html (accessed 6 May 2012).

[14] Peshko I. Self-effecting processes in the solid-state lasers. Honorary Dr. of Sciences dissertation. Institute of Physics Kiev; 2003.

[15] Tikhonov V I. Excesses of random processes. Moscow: Nauka; 1970. (in Russian).

[16] Wigner distribution function.
http://en.wikipedia.org/wiki/Wigner_distribution_function (accessed 6 May 2012).

[17] Sooy W. The natural selection of modes in a passive Q-switched laser. Appl.Phys.Lett. 1965; 2(6) 36-58.

[18] Peshko I, Khiznyak A, Soskin M. Mode-locked laser with controllable parameters. New York: Plenum-press; 1985. (Plenum Press bought the author's rights for initially published brochure: Peshko I, Khiznyak A, Soskin M. Laser of ultrashort pulses with tunable parameters. Kiev: Publishing of Institute of Physics, Academy of Sciences; 1984, #4).

[19] Peshko I, Khizhnyak A. Generation of the pulses of extreme short duration by solid-state lasers. Quantum Electronics 1987; 33, Kiev, Naukova Dumka p.14-20. (in Russian).

[20] Peshko I, Soskin M, Khiznyak A. Generation of the picosecond pulse train with controlable parameters. Quantum Electronics 1982; 9(12) 2391-2398. (in Russian).

[21] Graf F, Low C. Passively mode locked Nd-glass laser with partially suppressed natural mode selection. Opt. Communs. 1983; 47(5) 329-334.

[22] Becker M, Kuizenga D, Siegman A. Harmonic mode locking of the Nd:YAG laser. IEEE J. Quantum Electronics 1972; 8(8) 687-693.

[23] Encyclopedia of Laser Physics and Technology. Harmonic Mode Locking. http://www.rp-photonics.com/harmonic_mode_locking.html (accessed 6 May 2012).

[24] Zhan L. et al. Critical behavior of a passively mode-locked laser: rational harmonic mode locking. Opt. Lett. 2007; 32(16) 2276-xxx

[25] Attosecond pulse generation and detection www.mpq.mpg.de/lpg/research/attoseconds/attosecond.html (accessed 6 May 2012).

[26] Borot A, Malvache A, Chen X, Jullien A, Geindre J.-P, Audebert P, Mourou G, Quéré F, Lopez-Martens R. Attosecond control of collective electron motion in plasmas. Nature Physics 2012; 8 416-421.

[27] Zhu J, Xie X, Sun M, Bi Q, Kang J. A Novel Femtosecond laser System for Attosecond Pulse Generation. Advances in Optical Technologies 2012; Hindawi Publishing Corporation, article ID 908976, doi: 10.1155/2012/908976, 6 pages.

[28] Phys.Org.News. http://www.physorg.com/news192909576.html (accessed 6 May 2012).

[29] Lan P, Lu P, Cao W, Wang X. Attosecond and zeptosecond x-ray pulses via nonlinear Thomson backscattering. Phys. Rev. E 2005; 72, 066501[7 pages].

[30] Femtosecond, Attosecond, and Yoctosecond http://nextbigfuture.com/2009/10/attoseconds-zeptoseconds-and.html (accessed 10 May 2012).